

Article

A New Method of Quantitatively Evaluating Fracability of Tight Sandstone Reservoirs Using Geomechanics Characteristics and In Situ Stress Field

Liangbin Dou ^{1,2,3,*}, Xiongdi Zuo ^{1,2}, Le Qu ^{1,2}, Yingjian Xiao ⁴, Gang Bi ^{1,2}, Rui Wang ^{1,2} and Ming Zhang ^{1,2}

¹ School of Petroleum Engineering, Xi'an Shiyou University, Xi'an 710065, China; 19111010006@stumail.xsyu.edu.cn (X.Z.); qule@xsyu.edu.cn (L.Q.); big@xsyu.edu.cn (G.B.); rwang@xsyu.edu.cn (R.W.); zm9792@xsyu.edu.cn (M.Z.)

² Engineering Research Center of Development and Management for Low to Extra-Low Permeability Oil & Gas Reservoirs in West China, Ministry of Education, Xi'an 710065, China

³ Key Laboratory of Unconventional Oil & Gas Development, China University of Petroleum (East China), Ministry of Education, Qingdao 266580, China

⁴ School of Petroleum Engineering, Northeast Petroleum University, Daqing 163318, China; xiaoyj@nepu.edu.cn

* Correspondence: doulb@xsyu.edu.cn

Abstract: This paper studied the fracability of tight sandstone reservoirs by means of incorporating geomechanics properties and surrounding in situ stresses into a new model. The new fracability evaluation model consists of variables such as brittleness index, critical strain energy release rate index, horizontal stress difference, and minimum horizontal principal stress gradient. The probability of interconnection of a complex fracture network was quantitatively studied by the brittleness index and horizontal principal stress difference index. The probability of obtaining a large stimulated reservoir volume was evaluated by the critical strain energy release rate index and minimum horizontal principal stress gradient which also quantifies conductivity. This model is more capable of evaluating fracability, i.e., it agrees better with the history of production with a high precision and had correlation coefficients (R^2) of 0.970 and 0.910 with liquid production of post-fracturing well testing and the average production of six months of post-fracturing, respectively. It is convenient that all model inputs were obtained by means of loggings. Using this model, tight sandstone reservoirs were classified into three groups according to fracability: $\text{Frac} \geq 0.3 \text{ MPa}^{-1}\cdot\text{m}$ for Type-I, $0.22 \text{ MPa}^{-1}\cdot\text{m} \leq \text{Frac} < 0.3 \text{ MPa}^{-1}\cdot\text{m}$ for Type-II, and $\text{Frac} < 0.22 \text{ MPa}^{-1}\cdot\text{m}$ for Type-III.

Keywords: tight sandstone; fracability; brittleness; critical strain energy release rate; minimum horizontal principal stress; horizontal principal stress difference



Citation: Dou, L.; Zuo, X.; Qu, L.; Xiao, Y.; Bi, G.; Wang, R.; Zhang, M. A New Method of Quantitatively Evaluating Fracability of Tight Sandstone Reservoirs Using Geomechanics Characteristics and In Situ Stress Field. *Processes* **2022**, *10*, 1040. <https://doi.org/10.3390/pr10051040>

Academic Editor: Alessandro D'Adamo

Received: 31 March 2022

Accepted: 19 May 2022

Published: 23 May 2022

Publisher's Note: MDPI stays neutral with regard to jurisdictional claims in published maps and institutional affiliations.



Copyright: © 2022 by the authors. Licensee MDPI, Basel, Switzerland. This article is an open access article distributed under the terms and conditions of the Creative Commons Attribution (CC BY) license (<https://creativecommons.org/licenses/by/4.0/>).

1. Introduction

Tight sandstone reservoirs are characterized by low porosity and permeability. Thus, hydraulic fracturing is generally utilized to obtain a constant or large volume of single-well production [1]. The conventional hydraulic fracturing method is not applicable in the reservoirs. Volume fracturing in shale wells has become a critical technology in developing tight sandstone reservoirs. The fracturing operation sections have to be selected based on the optimization of the study of sweet spots. This rules out excessive operations. The selection of the fracturing sections is based on the precise and quantitative study of the fracability of reservoirs.

Generally, brittleness is taken as the major characteristic of evaluating the fracability of reservoirs. Li et al. [2] and Jin et al. [3] compiled over 20 methods of studying brittleness by statistical analysis. These methods mainly originate from specific issues that are applicable to different disciplines. There is no uniformity of these methods or standard testing methods. For hydraulic fracturing in unconventional reservoirs, a larger brittleness is commonly regarded to cause a higher brittleness index, and reservoirs are more easily

fractured and have higher productivities with a higher brittleness index. However, the brittleness index is incapable of characterizing the actual fracability of reservoirs. For some unconventional reservoirs, their elastic moduli and Poisson's ratios are comparable but their brittleness is significantly different. For other reservoirs, the brittleness index is high but it is difficult to be fractured [4,5]. It is unreliable or even inaccurate to evaluate the fracability of reservoirs solely by the brittleness index. Relying on the integration of different evaluation data to improve the accuracy of the model is already a reliable and verified means [6–8].

Following the study of brittleness, some researchers have proposed the terminology of fracability [9,10], in which the fracability corresponds to the ability of being fractured during hydraulic fracturing to improve productivity. Yuan et al. [11] built a fracability model by the integrating the brittleness index and fracture toughness. This model was introduced to tight sandstone reservoirs [1]. Jin et al. [3] built another fracability model based on brittleness by integrating fracture toughness and energy release rate and Young's modulus. Zhao et al. [12] proposed an evaluation method of fracability based on brittleness, fracture toughness, and natural fractures. Referring to the analytic hierarchy process, Sui et al. [13] studied the effect of rock properties on the fracability of shale, including brittleness, brittle mineral content, clay mineral content, cohesion, angle of internal friction, and unconfined compressive strength (UCS). Zhu and Carr [14] evaluated the effect of natural fractures and geomechanics on fracability. Wu et al. [15] studied the effect of brittleness, quartz content, diagenesis, and natural fractures on fracability. For the fracability of mud rock, Perera et al. [16] quantitatively analyzed the effect of the chemical content and saturation of reservoir fluids. For tight sandstone gas reservoirs, He et al. [17] studied the effect of brittleness, UCS, and mineral components on the fracability using the analytic hierarchy process. Ji et al. [18] proposed a fracability model based on the fractal theory and fracture toughness. Zhou et al. [19] proposed a new classification procedure to obtain the rock fracability index using the permeability index and brittleness index of rocks. Li et al. [20] evaluated fracability of the tight reservoir in the Junggar Basin based on the brittleness index, fracture toughness, and fracability index. Lu et al. [21] calculated the fracability index of deep shale based on gray correlation theory and the mechanical parameters, mineral composition, and stress-strain characteristics of shale.

From the literature review, there are two issues in the study of fracability of reservoirs. First, most studies neglect the effect of the surrounding stress field on fracability. Instead, they predominantly focus on rock properties of shale and tight sandstone reservoirs, i.e., geomechanics properties such as Young's modulus, Poisson's ratio, fracture toughness, UCS, or petrochemical properties such as mineral components and porous fluid saturation. Second, past fracability evaluation methods focus on the ease of the creation of a complex fracture network, but neglect the affecting factors on stimulated reservoir volume (SRV) and conductivity.

The success of hydraulic fracturing in tight reservoirs are dependent on geological properties, reservoir properties, and the operational process. Fracability is a comprehensive characteristic of hydraulic fracturing in tight reservoirs, which is irrelevant to the operational process. In this paper, fracability is defined as the ability to create and connect the complex fracture network, with maximized stimulated reservoir volume (SRV) and high conductivity, under the same or similar reservoir properties, fracturing scale, and operational process. To create the complex fracture network, requirements include large brittleness and adequate connection of hydraulic fractures and natural fractures in tight reservoirs. A relatively large SRV requires low energy consumption or small fracture toughness and the analytical effect of minimum horizontal principal stress for fracture propagation. Simultaneously, the minimum horizontal principal stress affects fracture closure pressure, and thus it influences the conductivity of fractures. In addition, a lower level of the minimum horizontal principal stress indicates a smaller confining pressure of reservoirs, larger brittleness [22,23], and higher fracability.

This paper proposes a new fracability model including geomechanics properties and in situ stress fields based on previous discussions. This model is capable of quantitatively evaluating the probability of the creation of complex fractures, showing the probability of acquiring a large SRV. Additionally, it is capable of evaluating the conductivity after hydraulic fracturing. The flow chart of the selection of fracability evaluation parameters is shown in Figure 1. The fracability evaluation method in this research aimed to increase the precision of studying fracability in tight sandstone reservoirs and improve the productivity of reservoir stimulation.

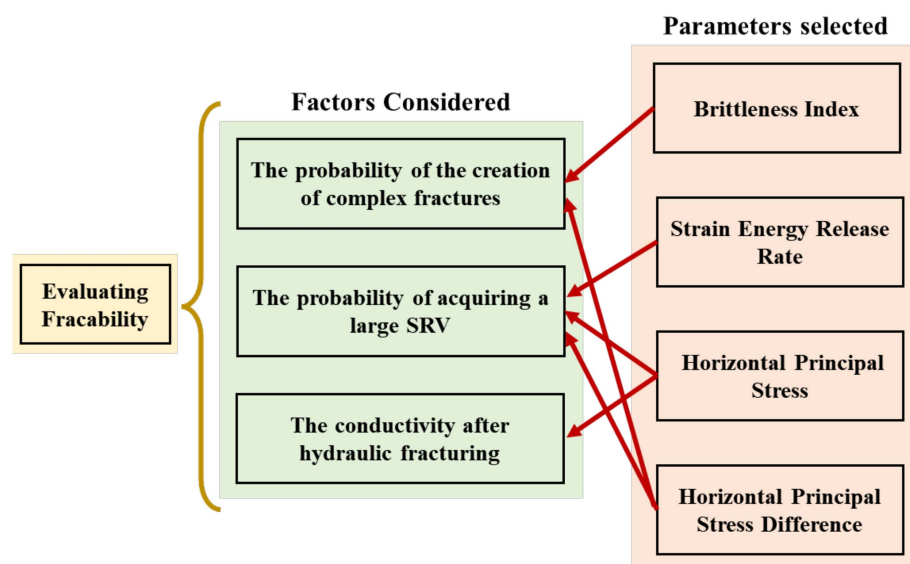


Figure 1. Flow chart of selection of the fracability evaluation parameters in this study, with arrows indicating that the parameters selected have an effect on the factors considered.

2. Analysis and Calculation of Fracability Evaluation Parameters

As shown in Figure 1, four fracability evaluation parameters, brittleness index, strain energy release rate, horizontal principal stress, and horizontal principal stress difference, were selected, and this section discusses the influence of each parameter in fracability evaluation and the calculation of their quantitative characteristic indices.

2.1. Brittleness Index

There are many ways of testing and evaluating brittleness which were compiled by Li et al. [2] and Jin et al. [3]. The majority of them have been proposed for different materials and specific problems such that they are applicable to various disciplines without uniformity. Standard testing methods have not yet been established. However, it is well-known that highly brittle rocks tend to fail at a small strain. Local fractures occur under inhomogeneous stresses resulting in multidimensional fracture planes to a large extent [2].

The emergence of many fracture planes characterizes large brittleness which is a macroscopic feature of fractures. Thus, larger brittleness causes more complex fractures during hydraulic fracturing in tight reservoirs. Some researchers have proposed the brittleness index which is used to characterize the complexity of fractures from hydraulic fracturing in tight rocks [24,25]. It is an essential parameter in studying the fracability of tight reservoirs.

Currently, brittleness index is commonly calculated from indoor core tests which are largely relevant to rock strength or rock failure, mineral component content tests, and geomechanics parameter tests [26]. Laboratory tests are commonly regarded to be more reliable, especially the geomechanics tests, in studying the brittleness of reservoirs. The disadvantages are inadequate cores due to limitations in time and cost, high testing expense, and long testing time. The mineral component content method utilizes the weight

percentage of brittle minerals over the overall tight reservoir rocks to characterize the brittleness index. However, this method is incapable of producing accurate evaluation results because of the lack of the diagenesis effect. The majority of field loggings do not include mineral content logging, and as a result, the brittleness index through the whole wellbore is not obtained.

The other more commonly used brittleness evaluation method is called the geomechanics parameter method, i.e., elastic parameters method, which was proposed by Grieser and Bray [27] and Rickman et al. [28]. It assumes that rock brittleness is mainly affected by elastic properties such as Young's modulus and Poisson's ratio. The brittleness of rock is larger when Young's modulus becomes larger and Poisson's ratio becomes smaller. Geomechanics properties are included in this method to characterize tight sandstone brittleness which are convenient to obtain. This method is more closely related to field applications which is more widely used. From their research, the brittleness index is described in Equation (1) [27,28].

$$BI = 0.5E_{Brit} + 0.5\mu_{Brit} \quad (1)$$

where, BI is the normalized brittleness index, dimensionless; E_{Brit} and μ_{Brit} are normalized Young's modulus and Poisson's ratio, respectively, dimensionless, and are defined as follows.

$$E_{Brit} = \frac{(E - E_{min})}{E_{max} - E_{min}} \quad (2)$$

$$\mu_{Brit} = \frac{(\mu_{max} - \mu)}{\mu_{max} - \mu_{min}} \quad (3)$$

where, E , E_{max} and E_{min} indicate static maximum and minimum Young's moduli of study areas, respectively, GPa; μ , μ_{max} , and μ_{min} are static, maximum, and minimum Poisson's ratios of study areas, dimensionless, respectively.

Static Young's modulus and Poisson's ratio are accessible through the empirical relations between dynamic logging data and the static data of indoor tests.

2.2. Strain Energy Release Rate

Based on dislocation behaviors, linear-elastic fracture mechanics assumes that fracture propagation is classified into three modes, i.e., opening (mode I), in-plane shear (mode II), and out-of-plane shear (mode III), as shown in Figure 2. A general fracture is a combination of the three basic types of fracture, producing compound fracture or mixed mode fracture. Mode I and II are the most common types of fracture in tight reservoir formations.

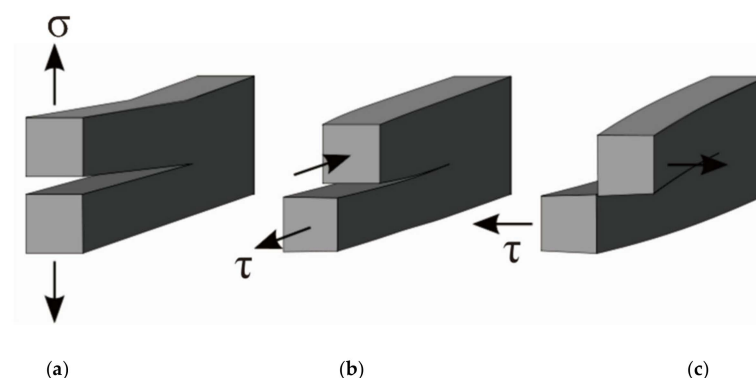


Figure 2. Three basic fracture modes of loading for a crack, σ is the normal stress and τ is the shear stress. (a) Mode I, (b) Mode II, and (c) Mode III.

Some researchers [29] established the fracture propagation criterion for I–II mixed mode fracture based on linear-elastic fracture mechanics. In hydraulic fracturing, the most commonly used fracture propagation criteria include the maximum tangential stress criterion, the maximum energy release rate criterion, and the minimum strain energy

density criterion. The maximum tangential stress criterion is simple since it solely examines the tensile stress as the cause of crack but neglects the effect of shearing stress. The minimum strain energy density criterion combines the energy of shearing and tensile. However, there are more inputs with complexity in this model than those in the maximum energy release rate criterion. The maximum energy release rate is simply but strongly correlated with stress intensity factors, which makes it convenient to conduct quantitative studies and which possesses great advantages over the other criteria. Thus, we adopted this criterion in this paper.

Of the fracture mechanics studies, Griffith [30] proposed the fracture propagation criterion based on the classical mechanics and the energy theory. Irwin [31] extended Griffith's energy balance theory by studying the balance relationship between added surface energy and released mechanical energy and proposing a reliable thermodynamics criterion about when the ideal brittle fracture propagates. Based on Griffith's criterion, Palaniswamy and Knauss [32] proposed the energy release rate criterion for mixed mode fracture, i.e., fracture tends to propagate in the direction of the maximum energy release rate. When the energy release rate reaches a critical value, fracture begins to propagate. Generally, with a smaller critical strain energy release rate (G_c), it is more favorable for hydraulic fractures to penetrate formation rocks under the same amount of energy input, producing a larger SRV. Based on Irwin [31] and Jin et al. [3], G_c is described in Equation (4) assuming G_c remains constant under conditions of various fracture modes.

$$G_c = K_{IC}^2 / (E / (1 - \nu^2)) \quad (4)$$

where, G_c is critical strain energy release rate, MPa·m; K_{IC} is fracture toughness of Mode I fracture; MPa·m^{0.5}; E is Young's modulus for reservoir formation, MPa; and ν is the Poisson's ratio of reservoirs, dimensionless.

Referring to the computational model of brittleness index, G_c is normalized and the resultant critical strain energy release rate index, i.e., G_c index, is calculated in Equation (5) [3,31].

$$G_{C-n} = \frac{(G_{C-max} - G_c)}{G_{C-max} - G_{C-min}} \quad (5)$$

where, G_{C-n} is normalized G_c , dimensionless; G_{C-max} and G_{C-min} are the maximum and minimum G_c , respectively, MPa·m.

In this paper, fracture toughness was calculated from a model proposed by Jin et al. [33] which is specific for tight sandstone and has been verified by many researchers. It is described in Equations (6)–(9).

$$K_{IC} = 0.0059S_t^3 + 0.0923S_t^2 + 0.517S_t - 0.3322 \quad (6)$$

$$S_t = (0.0045E_d(1 - V_{cl}) + 0.008V_{cl}E_d) / K \quad (7)$$

$$V_{cl} = \frac{2^{I_{GR} \cdot GCUR} - 1}{2^{GCUR} - 1} \quad (8)$$

$$I_{GR} = \frac{GR - GR_{min}}{GR_{max} - GR_{min}} \quad (9)$$

where, K_{IC} is Mode I fracture toughness, MPa·m^{0.5}; S_t is tensile strength, MPa; E_d is dynamic elastic modulus, MPa; V_{cl} is clay fraction, dimensionless; I_{GR} is the clay content index, dimensionless; GR , GR_{max} , and GR_{min} are gamma ray readings at target formations, pure shale, and clean sandstone, respectively, API; $GCUR$ is the Hilchie index, dimensionless, which is 3.7 for tertiary formation and 2.0 for older formations.

2.3. Minimum Horizontal Principal Stress and Horizontal Principal Stress Difference

In normal fault, the three principal stresses are denoted as σ_V , σ_H , and σ_h ($\sigma_V > \sigma_H > \sigma_h$). In reverse and strike-slip faults, the algebraically smallest of the three principal stresses is

referred to as the minimum principal stress in this paper. The principal stress difference is the intermediate stress minus the minimum principal stress.

2.3.1. Horizontal Principal Stress

To obtain a larger SRV, some other parameters have to be considered when the operations remain the same in hydraulic fracturing in tight sandstone. They are the critical strain energy release rate for fracture propagation and the effect of the minimum horizontal principal stress. It is easy for fractures to propagate when the minimum horizontal principal stress is at a low level, resulting in a larger SRV through hydraulic fracturing. This results in low levels of confining pressure and fracture closure pressure, relatively wide fractures, and relatively high conductivity.

The smaller value of minimum horizontal principal stress indicates a smaller confining pressure on reservoirs and larger brittleness of rocks. This effect is apparently large for low-strength tight reservoirs [22,34]. Additionally, minimum horizontal principal stress affects fracture toughness of reservoirs [23,33], i.e., a smaller minimum horizontal principal stress causes smaller values in fracture toughness and critical strain energy release rate, which benefits the propagation of fractures.

In this way, in situ stresses, particularly the minimum horizontal principal stress, directly influence the fracability of tight reservoirs. This is not negligible in evaluating fracability. Regarding the calculation of in situ stresses, many studies have been conducted and there are various methods [35–42]. This paper used the in situ stress calculation method from Song et al. [43] from loggings in tight sandstone reservoirs, which is based on horizontally homogeneous elastic factors. This method is described in Equations (10) and (11).

$$\sigma_h = \frac{E_H}{E_V} \frac{\nu_V}{1 - \nu_H} (\sigma_v - \alpha P_p) + \frac{E_H}{1 - \nu_H^2} \gamma + \frac{E_H \nu_H}{1 - \nu_H^2} \beta + \alpha P_p \quad (10)$$

$$\sigma_H = \frac{E_H}{E_V} \frac{\nu_V}{1 - \nu_H} (\sigma_v - \alpha P_p) + \frac{E_H}{1 - \nu_H^2} \beta + \frac{E_H \nu_H}{1 - \nu_H^2} \gamma + \alpha P_p \quad (11)$$

where, σ_v is overburden stress, MPa; σ_H, σ_h are maximum and minimum horizontal principal stresses, respectively, MPa; P_p is pore pressure, MPa; α is effective stress coefficient, dimensionless; E_V, E_H are vertical and horizontal Young's moduli, respectively, GPa; ν_V, ν_H are vertical and horizontal Poisson's ratio, dimensionless, respectively; and γ and β are tectonic stress coefficients at directions of minimum and maximum horizontal stresses, respectively, which are generally obtained from indoor rock tests in terms of the Kaiser's effect.

2.3.2. The Effect of Horizontal Principal Stress Difference

Natural fractures are generally well-developed in tight reservoirs. The occurrence of these fractures decreases rock strength and causes hydraulic fractures to initiate and propagate easily. More importantly, the complex fracture network is solely generated by the true connection of natural and hydraulic fractures resulting in a larger SRV.

Many studies have been conducted on the intersection of hydraulic and natural fractures, and the opening criteria of natural fractures and strike-slip [44–50]. Past research states that the intersection or connection between hydraulic and hydraulic fractures is mainly dependent on the approaching angle, horizontal principal stress difference (HSD), and strike angle. Natural fractures are distributed with extraordinary complexity inside tight sandstone reservoirs due to diagenesis, tectonic movement, and bedding. Currently, the delineation of formation fractures is feasible by means of borehole imaging technologies such as Fullbore Formation Microimager (FMI) or acoustic image logging. Unfortunately, they are high in cost but low in precision and unable of precisely and quantitatively delineate the development, azimuth, and strike of natural fractures within tight reservoirs. Comparatively, in situ stresses are able to be measured using existing developed technologies with high precision. Referring to in situ stress difference, this paper quantitatively studied the effective connection of natural fractures to form a complex fracture network

due to the generation of hydraulic fractures. The former studies indicate that low and intermediate levels of horizontal principal stress difference facilitate the connection of hydraulic and natural fractures. Simultaneously, hydraulic fractures swell or initiate, producing a complex hydraulically induced fracture network. Under a large horizontal principal stress difference, hydraulic fractures vertically penetrate natural fractures which results in a single major fracture instead of a fracture network. The horizontal principal stress difference significantly influences the initiation and propagation of a complex fracture network.

Cheng et al. [50,51] conducted hydraulic fracturing tests on rock samples with preset natural fractures and discontinuities using a true triaxial compression instrument. The results showed a critical value in horizontal principal stress difference, i.e., 5–7 MPa, as demonstrated in Figure 3. Above this critical value, hydraulic fractures directly connect natural fractures which produce simple planar fractures. Under this value, re-orientation and propagation occur when hydraulic and natural fractures intersect, regardless of the occurrence of natural fractures. Then, natural fractures are well-interconnected with the complex fracture network which increases the SRV.

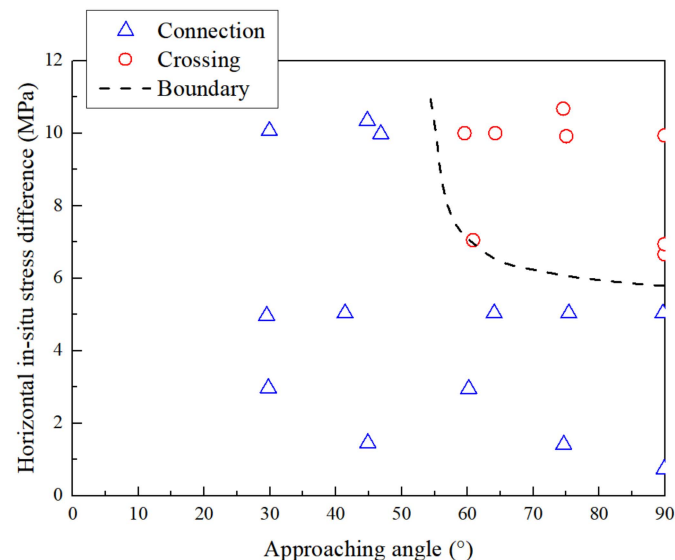


Figure 3. Influences of horizontal in situ stress difference and approaching angle on fracture propagation. ‘Connection’ indicates that hydraulic fractures and natural fractures are interconnected, and natural fractures are ultimately extended by the intersected hydraulic fractures. ‘Crossing’ indicates that natural fractures are crossed by hydraulic fractures without interconnection.

The horizontal principal stress difference is as small as possible to reach complex and large volume of fracture network in tight sandstone reservoirs. This facilitates the connection of hydraulic and natural fractures. The HSD index is defined in Equation (12).

$$S_N = 1 - \frac{\Delta\sigma}{\Delta\sigma_{\max}} \quad (12)$$

where, S_N is the normalized HSD index, dimensionless; $\Delta\sigma$, $\Delta\sigma_{\max}$ are actual and maximum HSD, respectively, MPa.

$$\Delta\sigma = \sigma_H - \sigma_h \quad (13)$$

where, σ_H and σ_h are maximum and minimum horizontal principal stresses, respectively, MPa.

The maximum HSD is accessible from statistical analysis on reservoir HSD. Alternatively, it was regarded to be 7 MPa referring to compiled experimental results [50]. If the actual value in $\Delta\sigma$ was over 7 MPa, this value was taken into calculation.

3. New Model for Fracability Evaluation

From hydraulic fracturing, only those fractures with more complexity and larger SRV are of economic value and have relatively high production capacity. In this way, the purpose of evaluating tight sandstone fracability is to quantitatively evaluate the probability of complex fractures with a large SRV.

The complexity of the induced fracture network is quantitatively evaluated mainly by the brittleness index and HSD. The size of SRV is mainly determined by the G_c index and minimum horizontal principal stress. The conductivity of induced fractures is characterized by the minimum horizontal principal stress gradient. It is worth mentioning that HSD influences SRV, i.e., a smaller value in HSD causes more complexity in the induced fracture network and a larger SRV.

In tight sandstone reservoirs, a new fracability evaluation model with normalization consists of variables such as the comprehensive brittleness index (BI), HSD index (S_N), G_c index (G_{C-N}), and minimum horizontal principal stress gradient (σ_h^G), and the calculation flow chart is shown in Figure 4.

$$F_{rac} = (\alpha \cdot BI + \beta \cdot G_{C-N} + \gamma \cdot S_N) / \sigma_h^G \quad (14)$$

where $\alpha + \beta + \gamma = 1$.

where, F_{rac} is the fracability index, $\text{MPa}^{-1} \cdot \text{m}$; σ_h^G is the minimum horizontal principal stress gradient, $\text{MPa}/100 \text{ m}$; α , β , and γ are brittleness index (BI), G_c index (G_{C-N}) and HSD index (S_N), dimensionless, respectively. The α and γ are increased to meet the priority requirement of induced fracture complexity, otherwise β is increased for a larger SRV. The appropriate values of α , β , and γ should be chosen according to the purpose. In this paper, α , β , and γ took the values of 0.33, 0.33, and 0.34, respectively.

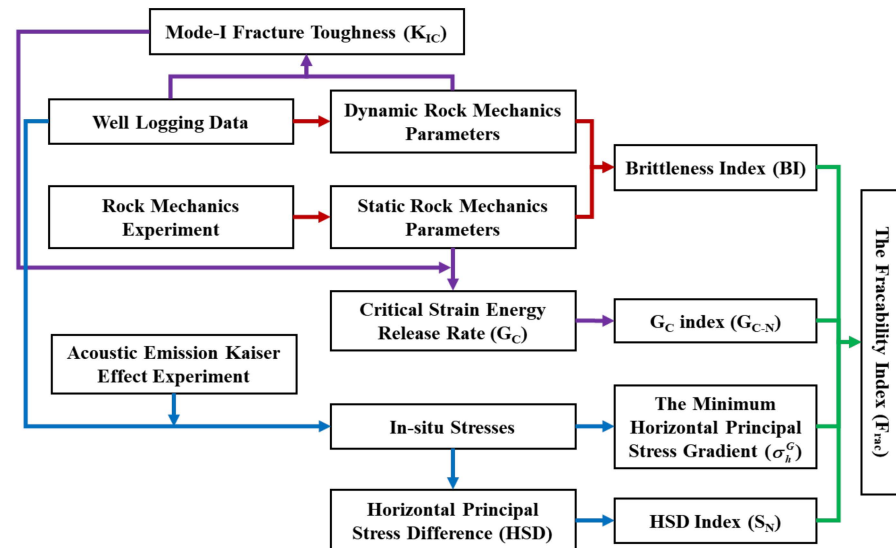


Figure 4. Flow chart of the calculation of each parameter in the fracability index (F_{rac}) model.

4. Case Study and Comparative Analysis

This paper studied the fracability evaluation of the Chang-6 Formation of the Heshui Region, Ordos Basin, China. The main sedimentary face is delta deposit where sand bodies are well-developed. The reservoir rocks are sandstone or siltstone with quartz, with feldspars and lithic fragments as the major sandstone particles. The portion of interstitial materials are low and they are mainly argillaceous matrix and cements. The major brittle minerals, i.e., quartz and carbonate, comprise more than 60% of the overall weight. The reservoir properties are poor. For example, the porosity ranges from 6% to 17% with an average of 8.8% and the permeability is in the range of 0.01 mD~2.4 mD with an average of 0.32 mD. The reservoir is characterized as having extremely low porosity and

permeability [52,53]. Natural fractures are well-developed as observed in reservoir cores (Figure 5), which benefit the interconnection between hydraulic and natural fractures and the generation of a complex fracture network.

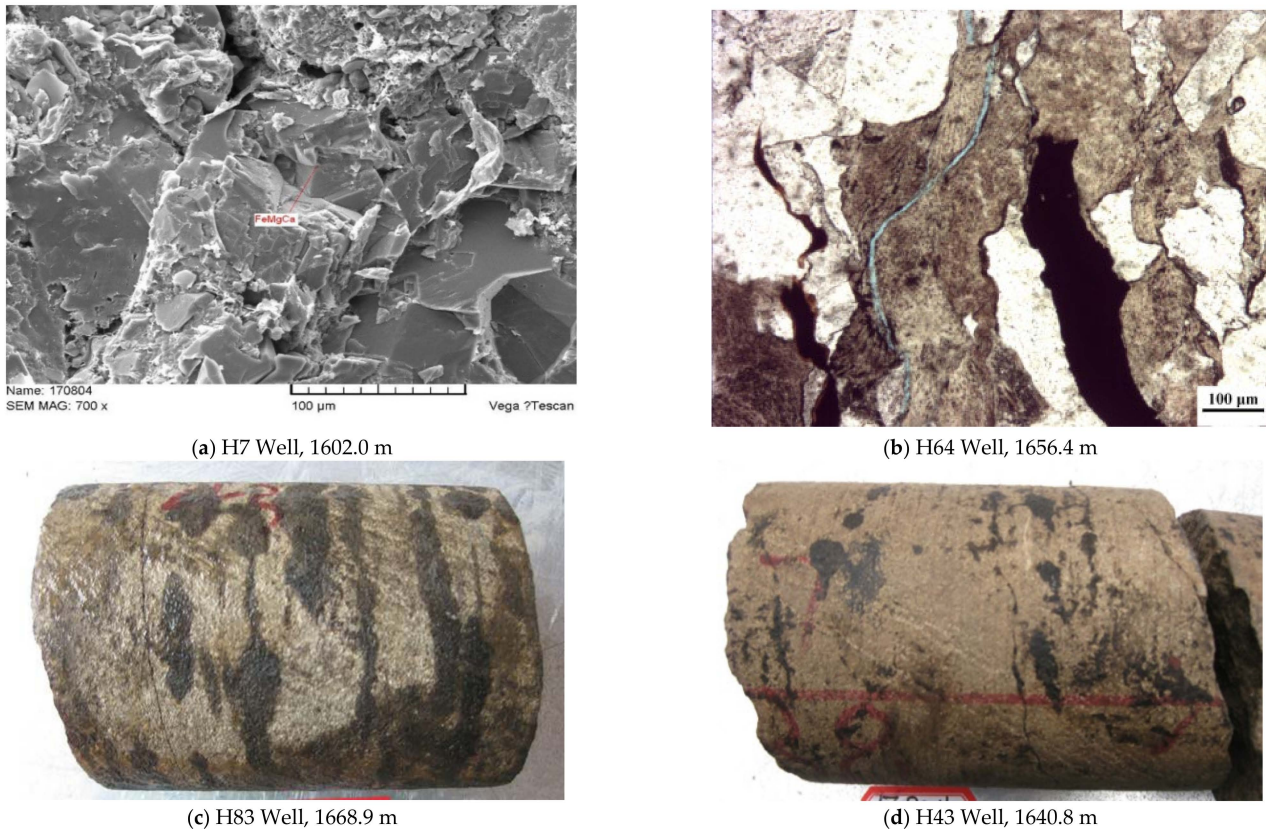


Figure 5. Natural fractures are well-developed in tight sandstone cores, which were obtained from the Heshui Region of Ordos Basin, China. (a) was obtained from the scanning electron microscopy (SEM) test. (b) was obtained from the thin section petrography (TSP) test. (c,d) are images of whole core retrieved from H83 Well and H43 Well, respectively.

This paper studied three adjacent wells (H64, H7, and H83) in Chang-6 Formation of the Heshui Region. They are representative of this area and prerequisite conditions were similar for each other, i.e., reservoir properties such as porosity and permeability, fracturing scale, and fracturing techniques. A significant difference in production was observed from the three wells after hydraulic fracturing was finished, as shown in Table 1, of which the most influential factor was reservoir fracability. In Figures 6–8, some parameters of the three wells were obtained such as geomechanics properties, in situ stresses, fracture toughness, and the fracability index. They were obtained by the integration of logging data and indoor experiments. For example, tectonic stress coefficients were calculated from monitoring acoustic emissions through in situ stress experiments in terms of Kaiser’s effect. From the response of stress–strain under triaxial stresses, statistical data of rocks in this area showed that Young’s moduli were 2.5 GPa larger in the horizontal direction than those in vertical direction, and that Poisson’s ratios were almost identical in both directions. Through triaxial in situ stress and acoustic emission measurement tests, correlations were built between dynamic and static parameters for both Young’s modulus and Poisson’s ratio. In these figures, rectangular areas enclosed with dashed lines indicate the actual heights of hydraulically induced fractures. This was obtained by the comparison analysis of inhomogeneity of reservoirs before and after hydraulic fracturing.

From Table 1 and Figure 6, the BI values of fractured sections in Well H64 were in the range of 0.46–0.58 with a mean value of 0.49; Gc-n ranged from 0.14 to 0.43 with an average

value of 0.35; horizontal principal stress difference ranged from 4.9 to 6.8 MPa with an average of 5.5 MPa; HSD index ranged from 0.05 to 0.31 with an average of 0.22; minimum horizontal principal stress gradient ranged from 1.78 to 2.04 MPa/100 m with an average of 1.86 MPa/100 m; and fracability ranged from 0.13 to 0.22 MPa⁻¹·m with an average of 0.19 MPa⁻¹·m.

The BI in fractured sections of Well H64 was large where it was small in Gc-n. This made it difficult to obtain a relatively large SRV. The horizontal principal stress difference was large and it was also large in the minimum horizontal principal stress gradient, which indicated poor interconnection of hydraulic and natural fractures. This prohibits the propagation of fractures, causing low productivity.

From Table 1 and Figure 7, the BI values of fractured sections in Well H7 were in the range of 0.39~0.48 with a mean value of 0.42; Gc-n ranged from 0.36 to 0.58 with an average value of 0.51; horizontal principal stress difference ranged from 2.0 to 3.0 MPa with an average of 2.3 MPa; HSD index ranged from 0.57 to 0.71 with an average of 0.66; minimum horizontal principal stress gradient ranged from 1.59 to 1.74 MPa/100 m with an average of 1.62 MPa/100 m; and fracability ranged from 0.30 to 0.40 MPa⁻¹·m with an average of 0.36 MPa⁻¹·m.

The BI in fractured sections of Well H7 was small where it was large in Gc-n. This made it easy to obtain a relatively large SRV. The horizontal principal stress difference was small and it was also small in the minimum horizontal principal stress gradient, which indicated good interconnection of hydraulic and natural fractures. Then, a complex fracture network was generated and it tended to propagate with a small fracture closure pressure and high conductivity. In this way, the test productivity was high and it was capable of obtaining a relatively large production.

From Table 1 and Figure 8, the BI values of fractured sections in Well H83 were in the range of 0.41~0.51 with a mean value of 0.44; Gc-n ranged from 0.35 to 0.70 with an average value of 0.59; horizontal principal stress difference ranged from 2.8 to 5.3 MPa with an average of 3.9 MPa; HSD index ranged from 0.24 to 0.59 with an average of 0.44; minimum horizontal principal stress gradient ranged from 1.53 to 1.93 MPa/100 m with an average of 1.72 MPa/100 m; and fracability ranged from 0.19 to 0.36 MPa⁻¹·m with an average of 0.29 MPa⁻¹·m.

Table 1. Comparison of reservoir physical properties, fracturing process, and production results of three wells in Chang 6 pay zone.

Well		H64	H7	H83
Reservoir physical properties	Porosity (%)	8.3	8.8	9.5
	Intrinsic permeability (mD)	0.269	0.285	0.301
	Saturation of movable fluid (%)	60.54	58.17	55.43
Fracturing operational parameters	Fracturing fluid	Slickwater	Slickwater	Slickwater
	Amount of sand (m ³)	90.0	90.0	100.0
	Sand concentrations (%)	9.0	9.5	9.1
	Displacement (m ³ /min)	1.2 + 3.8	1.2 + 3.8	1.2 + 3.8
	Fracture height (m)	1631–1659	1605–1631	1479–1504
Fracability	BI	0.49	0.43	0.44
	BK	0.39	0.47	0.47
	BG	0.43	0.48	0.49
	Frac (MPa ⁻¹ ·m)	0.18	0.36	0.29
Production	Liquid production of post-fracturing well testing (m ³ /d), water cut (%)	14.2, 0	33.9, 0	28.4, 0
	The average production of six months of post-fracturing (m ³ /d), water cut (%)	0.89, 58.6%	2.42, 41.3%	1.54, 54.8%

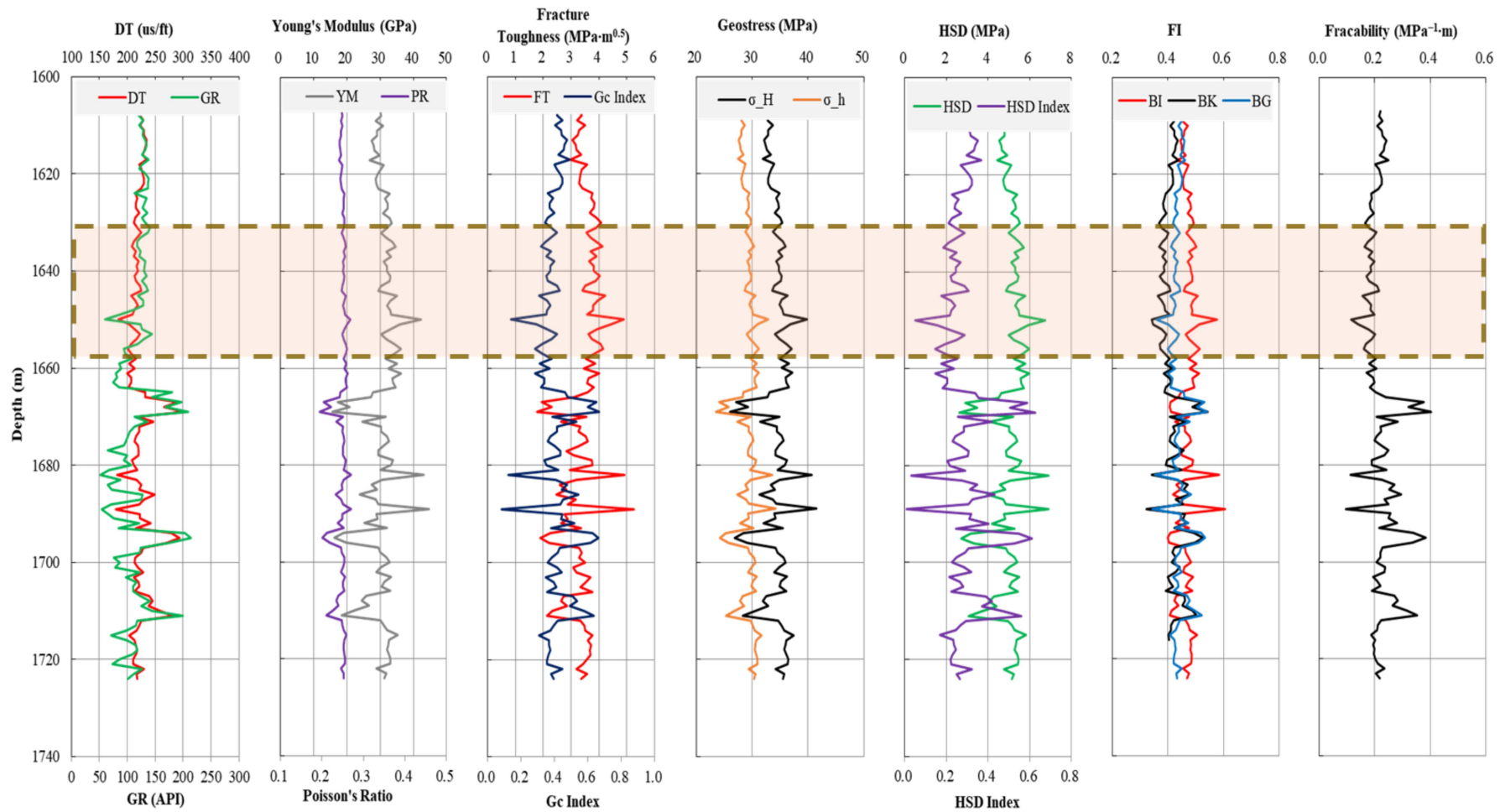


Figure 6. Profiles of fracability and other key parameters from Well H64.

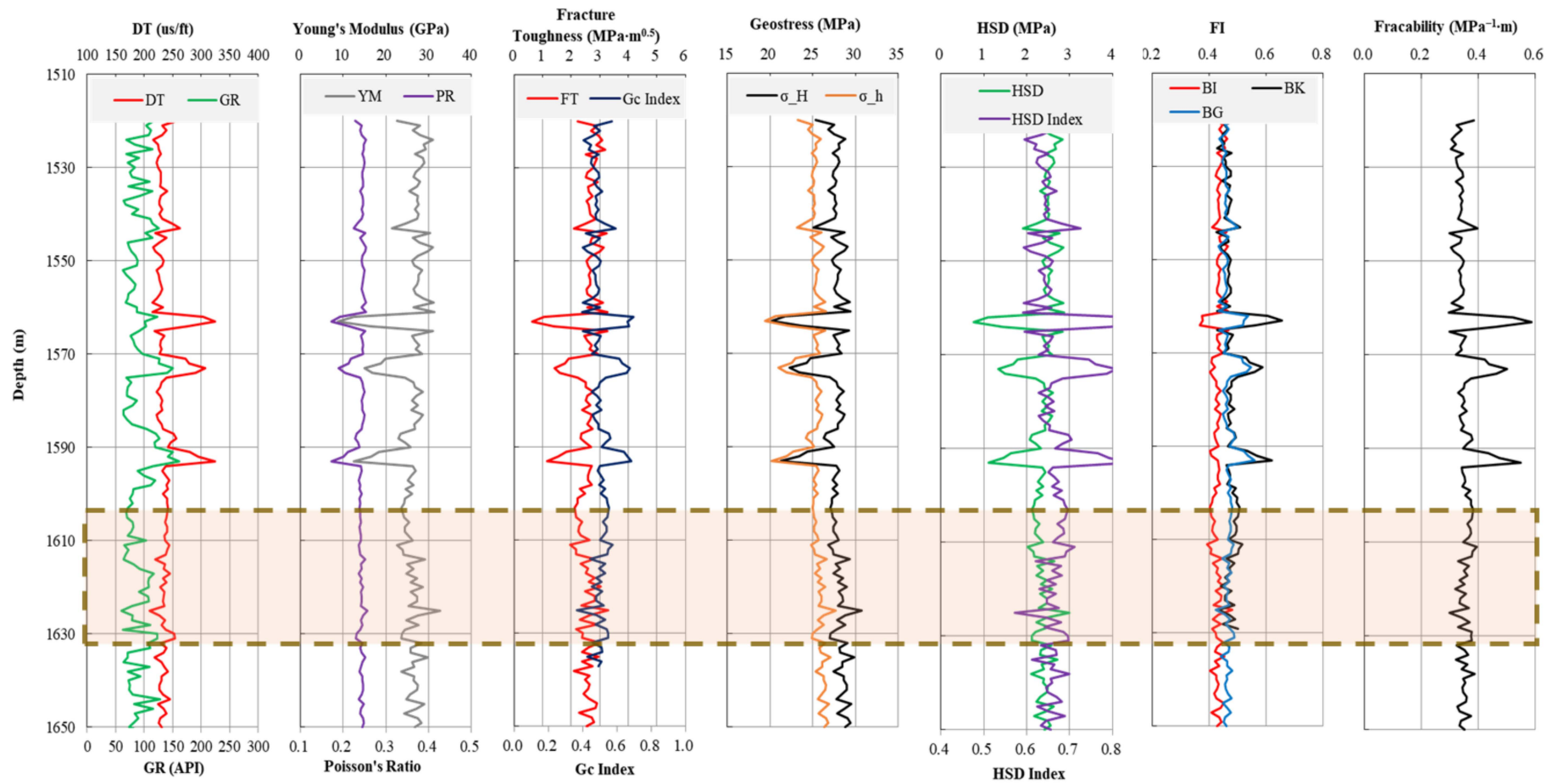


Figure 7. Profiles of fracability and other key parameters from Well H7.

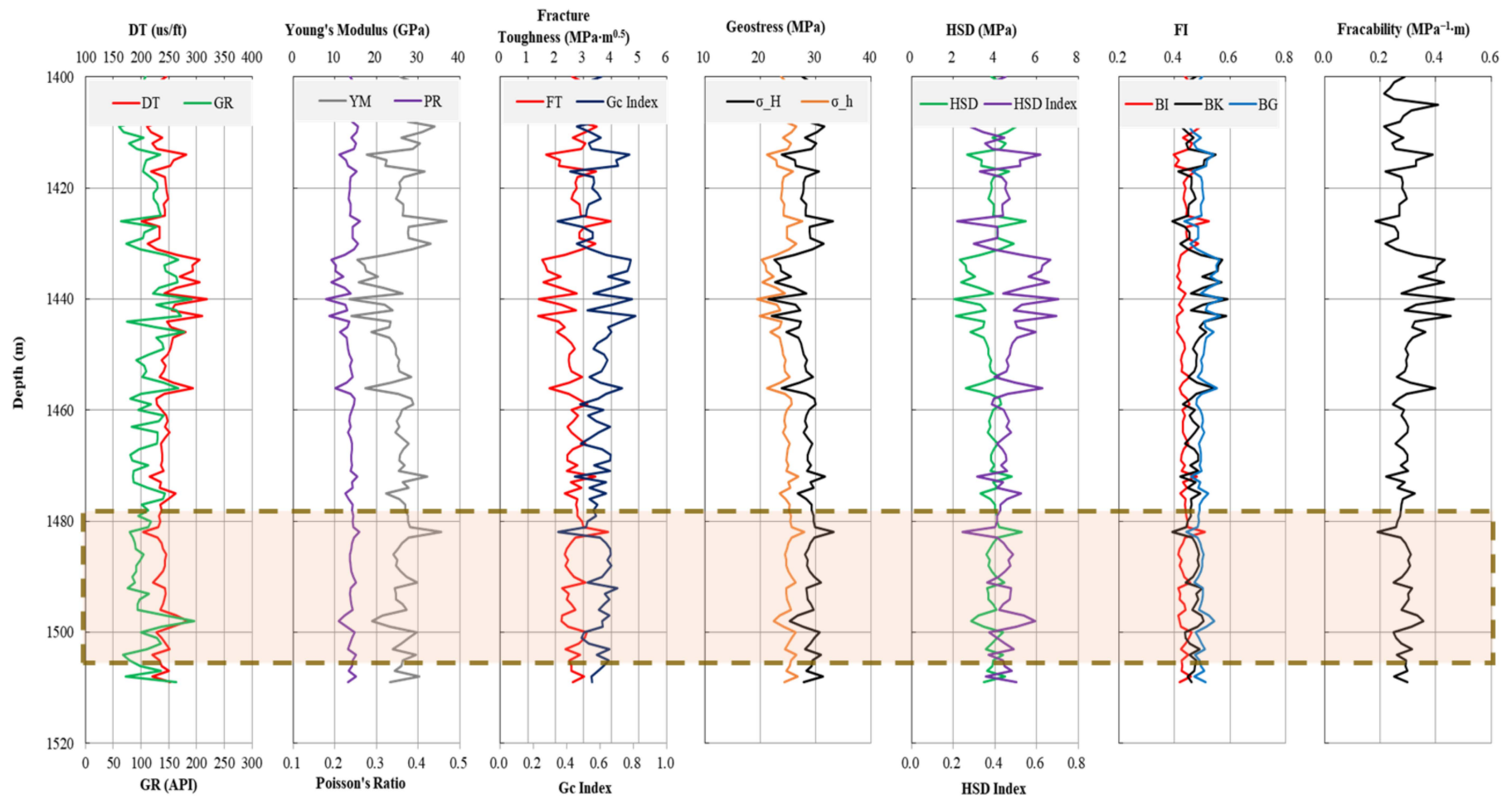


Figure 8. Profiles of fracability and other key parameters from Well H83.

The BI in fractured sections of Well H83 was intermediate where it was large in Gc-n. This made it easy to obtain a relatively large SRV. The horizontal principal stress difference was intermediate and it was also intermediate in the minimum horizontal principal stress gradient, which indicated inadequate interconnection of hydraulic and natural fractures. This showed that the fracability and production were at a moderate level.

There have been several fracability evaluation models such as the classical brittleness index model (BI), the integration model of brittleness index and critical strain energy release rate index (BG), and the integration model of brittleness index and fracture toughness index (BK). They were compared with our fracability model in this paper and listed in Table 1 and Figures 6–9. Specifically, the compiled fracability parameters of fractured sections are demonstrated in Figure 9.

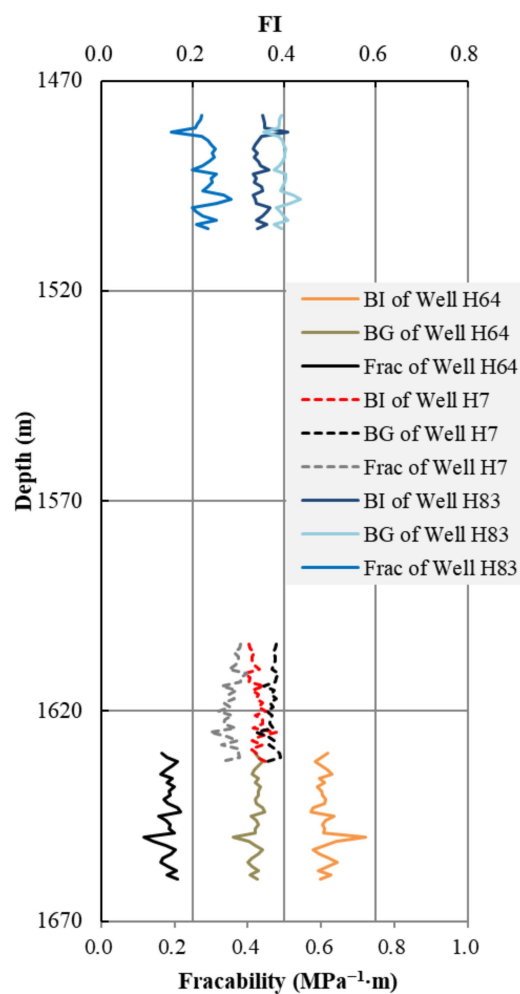


Figure 9. The fracability results of fractured sections from the three wells were compiled separately for better comparison.

The formula of BI [27,28] is expressed in Equation (1). Expressions of BG [3] and BK [3,12] are shown in Equations (15) and (16), respectively.

$$BG = 0.5 \cdot BI + 0.5 \cdot G_{C-N} \quad (15)$$

$$BK = 0.5 \cdot BI + 0.5 \cdot K_{IC-N} \quad (16)$$

$$K_{IC-N} = \frac{K_{ICmax} - K_{IC}}{K_{ICmax} - K_{ICmin}} \quad (17)$$

where, BI is the brittleness index, as described in Equation (1); K_{IC-N} is the fracture toughness index, dimensionless; and K_{ICmax} and K_{ICmin} are the maximum and minimum fracture toughness, respectively, $MPa \cdot m^{0.5}$.

From Table 1 and Figure 9, the brittleness index was incapable of characterizing the fracability of tight sandstone reservoirs under similar reservoir properties, fracturing scale, and operational process of the three wells. For example, Well H64 had the largest brittleness index while the production of post-fracturing was the lowest. Well H7 had a small brittleness index while its production of post-fracturing was the highest. In this way, the brittleness index of reservoirs solely indicates that multidimensional fracture faces are easily generated with variation in fracture faces under the same conditions.

Brittleness index is a basis to derive some fracability models. For example, the BK fracability model is generated by the combination of the brittleness index and normalized fracture toughness index, and the BG model is formed from the combination of the brittleness index and normalized G_c index. These fracability models solely consider reservoir rock properties, and as a result, there is little difference in the resultant fracability index values [26]. This makes it difficult to recognize fracture sweet spots. For example, the fracability index values were close in both BK and BH models for wells H7 and H64. They were incapable of accurately characterizing reservoir fracability.

These fracability models, i.e., BI, BG, and BK only consider the reservoir rock properties, failing to consider the effect from the in situ stress field. In this way, the effective fracability model with a high precision has to incorporate the surrounding in situ stress field along with the reservoir rock properties. The horizontal principal stress difference and HSD index are used to characterize the favorable interconnection between natural and hydraulic fractures. The minimum horizontal principal stress gradient is used to characterize the propagation of open fractures and the conductivity after hydraulic fracturing. Our fracability model was capable of differentiating the fracability of cross-hole areas and various sections within a well. This model agrees well with the production data which verifies its accuracy. All inputs are accessible from logging while some of them might require calibration with the help of conventional laboratory tests. This benefits the recognition of fracture sweet spots of reservoirs in the field.

The correlations between the corresponding index and history of production for the different models were calculated, and as can be seen in Figure 10, the BI, BG, and BK indices correlated better with liquid production of post-fracturing well testing, with correlation coefficients (R^2) of 0.972, 0.652, and 0.854, respectively, but the correlation with the average production of six months of post-fracturing became significantly worse; in particular, the correlation coefficient between the BG index and the average production of six months of post-fracturing was only 0.038. However, our Frac model correlated well with both liquid production of post-fracturing well testing and the average production of six months of post-fracturing, with R^2 of 0.970 and 0.910, respectively.

Using the fracability model in this paper, fracability data were obtained and statistical analysis of them indicated three types of reservoirs in terms of fracability. Classifications of reservoirs are detailed as follows.

- (1) Type-I: $Frac \geq 0.3 MPa^{-1} \cdot m$. For this type, there was a high probability of obtaining a complex fracture network, a greater SRV, and high conductivity. The fracability was ranked high.
- (2) Type-II: $0.22 MPa^{-1} \cdot m \leq Frac < 0.3 MPa \cdot m$. For this type, there was an intermediate probability of obtaining a complex fracture network and a greater SRV. The fracability was ranked intermediate.
- (3) Type-III: $Frac < 0.22 MPa^{-1} \cdot m$. For this type, it was difficult to obtain a complex fracture network and a greater SRV. The fracability was ranked low and hydraulic fracturing is not advised for this type of reservoirs.

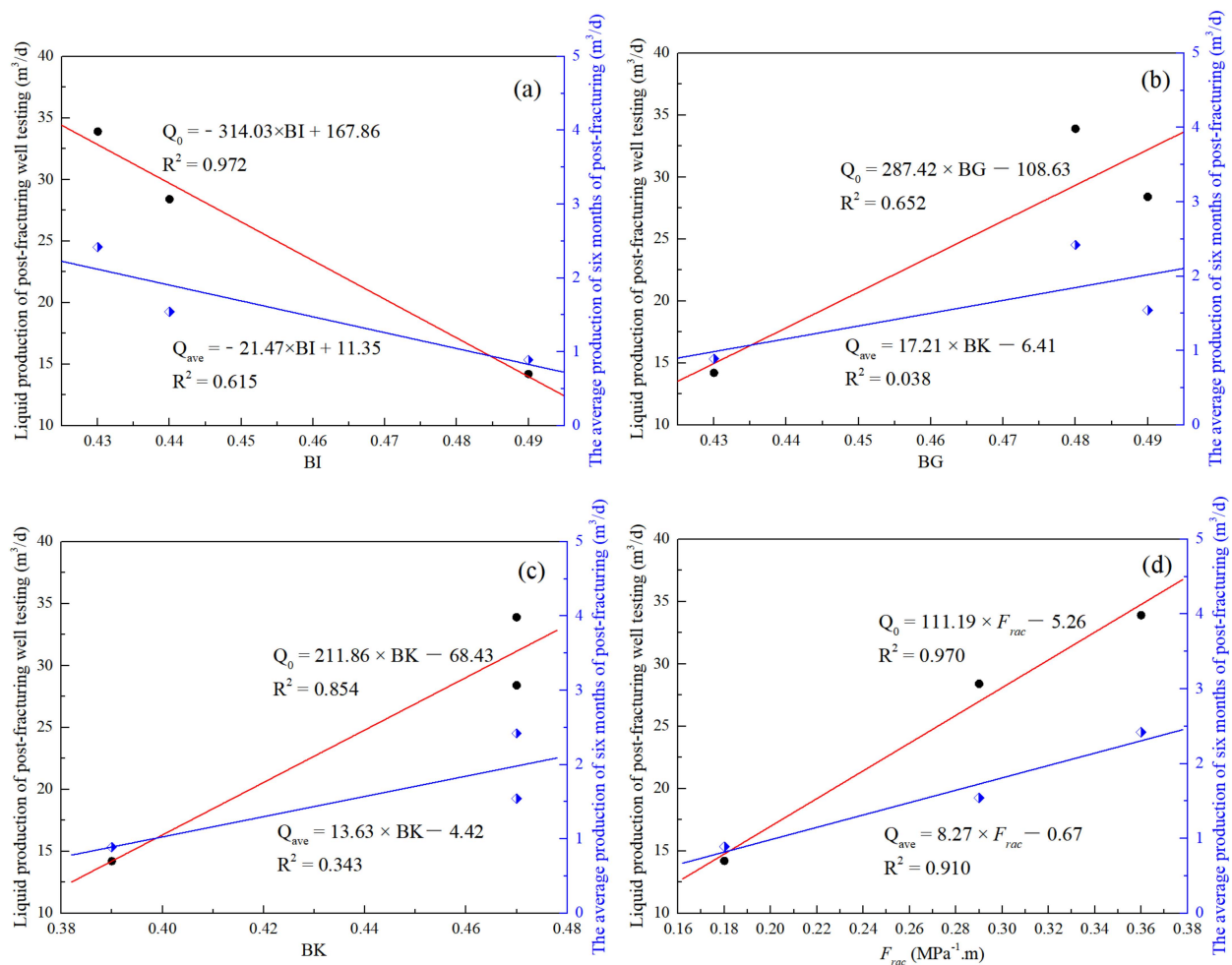


Figure 10. The correlations between the corresponding index and history of production for (a) BI model, (b) BG model, (c) BK model, and (d) F_{rac} model.

5. Conclusions

In tight sandstone reservoirs, good fracability refers to the ability to obtain relatively high productivity under the same or similar reservoir properties, fracturing scale, and operational process. This paper proposed three requirements for high productivity in sandstone reservoirs. First, reservoirs are capable of generating a complex fracture network. Second, induced fractures can make a large SRV. Third, the conductivity is high for the induced fracture network. Following these ideas, this research studied fracability in tight reservoirs by incorporating the effects of geomechanics properties and surrounding in situ stresses on fracture propagation and closure.

A new fracability evaluation model was built for tight sandstone reservoirs. It consists of variables such as brittleness index, critical strain energy release rate index, horizontal principal stress difference, and minimum horizontal principal stress gradient. The probability of the generation of a complex fracture network was quantitatively studied by the brittleness index and horizontal principal stress difference index. The probability of obtaining a large SRV was evaluated by the critical strain energy release rate index and minimum horizontal principal stress gradient which is also capable of quantifying conductivity. Therefore, the fracability model covers all the aspects of obtaining high efficiency and a complex fracture network.

Our new fracability model agrees well with the history of production with showed high precision through the study of fracability and productivity in tight sandstone reservoirs of Chang-6 Formation of the Heshui Region, Ordos Basin, China. It improves some of the issues of past fracability models that only consider geomechanics properties of

reservoirs. In addition, all model inputs were capable of being obtained through loggings. This makes it easy to be applied in the field. Using this model along with statistical analysis, tight sandstone reservoirs were classified into three groups in terms of fracability: $\text{Frac} \geq 0.3 \text{ MPa}^{-1} \cdot \text{m}$ for Type-I, $0.22 \text{ MPa}^{-1} \cdot \text{m} \leq \text{Frac} < 0.3 \text{ MPa}^{-1} \cdot \text{m}$ for Type-II, and $\text{Frac} < 0.22 \text{ MPa}^{-1} \cdot \text{m}$ for Type-III.

The fracability model in this paper considers the effect of in situ stress on reservoir rocks. This new development improves the accuracy of studying fracability for tight sandstone reservoirs. The model is also instructive to evaluate fracability for other unconventional reservoirs such as shale gas, shale oil, and coal bed methane. However, our fracability model does not consider the effect of the degree of microfracture development due to the current difficulty in obtaining microcrack monitoring data (e.g., lack of imaging logging data in the study area) and accurately and quantitatively characterizing the degree of microcrack development. With the advancement of technology, it can be further improved in the future.

Author Contributions: Conceptualization, L.D. and X.Z.; Methodology, Y.X. and L.Q.; Validation, L.Q., G.B. and R.W.; Formal analysis, G.B. and M.Z.; Investigation, G.B. and Y.X.; Data curation, M.Z. and L.Q.; Writing—original draft preparation, X.Z. and Y.X.; Writing—review and editing, L.D. and X.Z.; Supervision, R.W.; Project administration, L.D. and M.Z.; Funding acquisition, L.D. and L.Q. All authors have read and agreed to the published version of the manuscript.

Funding: This research was financially supported by the National Natural Science Foundation of China (No. 52074221, 52074224, 52004223 and 52020105001) and the Foundation of Key Laboratory of Unconventional Oil & Gas Development (China University of Petroleum (East China)) (No. 19CX05005A-203).

Conflicts of Interest: The authors declare no conflict of interest.

References

1. Sun, J.M.; Han, Z.L.; Qin, R.B.; Zhang, J.Y. Log evaluation method of fracturing performance in tight gas reservoir. *Acta Pet. Sin.* **2015**, *36*, 74–80.
2. Li, Q.H.; Chen, M.; Jin, Y.; Wang, F.P.; Hou, B.; Zhang, B.W. Indoor evaluation method for shale brittleness and improvement. *Chin. J. Rock Mech. Eng.* **2012**, *31*, 1680–1685.
3. Jin, X.; Shah, S.N.; Roegiers, J.C.; Zhang, B. An integrated petrophysics and geomechanics approach for fracability evaluation in shale reservoirs. *SPE J.* **2015**, *20*, 518–526. [[CrossRef](#)]
4. Wang, X.; Ge, H.; Wang, D.; Wang, J.; Chen, H. A comprehensive method for the fracability evaluation of shale combined with brittleness and stress sensitivity. *J. Geophys. Eng.* **2017**, *14*, 1420–1429. [[CrossRef](#)]
5. Bai, M. Why are brittleness and fracability not equivalent in designing hydraulic fracturing in tight shale gas reservoirs. *Petroleum* **2016**, *2*, 1–19. [[CrossRef](#)]
6. Shahbazi, A.; Monfared, M.S.; Thiruchelvam, V.; Fei, T.K.; Babasafari, A.A. Integration of knowledge-based seismic inversion and sedimentological investigations for heterogeneous reservoir. *J. Asian Earth Sci.* **2020**, *202*, 104541. [[CrossRef](#)]
7. Soleimani, M.; Jodeiri Shokri, B.; Rafiei, M. Integrated petrophysical modeling for a strongly heterogeneous and fractured reservoir, Sarvak Formation, SW Iran. *Nat. Resour. Res.* **2017**, *26*, 75–88. [[CrossRef](#)]
8. Soleimani, M.; Jodeiri Shokri, B. 3D static reservoir modeling by geostatistical techniques used for reservoir characterization and data integration. *Environ. Earth Sci.* **2015**, *74*, 1403–1414. [[CrossRef](#)]
9. Chong, K.K.; Grieser, W.V.; Passman, A.; Tamayo, C.H.; Modeland, N.; Burke, B. A Review of Successful Approach Towards Shale Play Stimulation in the Last Two Decades. In Proceedings of the Canadian Unconventional Resources and International Petroleum Conference, Calgary, AB, Canada, 19–21 October 2010. SPE-133874-MS.
10. Tang, Y.; Xing, Y.; Li, L.Z.; Zhang, B.H.; Jiang, S.X. Influence factors and evaluation methods of the gas shale fracability. *Earth Sci. Front.* **2012**, *19*, 356–363.
11. Yuan, J.L.; Deng, J.G.; Zhang, D.Y.; Li, D.; Yan, W.; Chen, C.; Chen, L.; Chen, Z. Fracability evaluation of shale-gas reservoirs. *Acta Pet. Sin.* **2013**, *34*, 523–527.
12. Zhao, J.Z.; Xu, W.J.; Li, Y.M.; Hu, J.Y.; Li, J.Q. A new method for fracability evaluation of shale-gas reservoirs. *Nat. Gas Geosci.* **2015**, *26*, 1165–1172.
13. Sui, L.; Ju, Y.; Yang, Y.; Yang, Y.; Li, A. A quantification method for shale fracability based on analytic hierarchy process. *Energy* **2016**, *115*, 637–645. [[CrossRef](#)]
14. Zhu, Y.; Carr, T.R. Estimation of fracability of the Marcellus shale: A case study from the MIP3H in Monongalia county, West Virginia, USA. In Proceedings of the SPE/AAPG Eastern Regional Meeting, Pittsburgh, PA, USA, 7–11 October 2018. SPE-191818-18ERM-MS.

15. Wu, J.; Zhang, S.; Cao, H.; Zheng, M.; Sun, P.; Luo, X. Fracability evaluation of shale gas reservoir-A case study in the Lower Cambrian Niutitang formation, northwestern Hunan, China. *J. Pet. Sci. Eng.* **2018**, *164*, 675–684. [[CrossRef](#)]
16. Perera, M.S.A.; Sampath, K.H.S.M.; Ranjith, P.G.; Rathnaweera, T.D. Effects of pore fluid chemistry and saturation degree on the fracability of Australian warwick siltstone. *Energies* **2018**, *11*, 2795. [[CrossRef](#)]
17. He, R.; Yang, Z.; Li, X.; Li, Z.; Liu, Z.; Chen, F. A comprehensive approach for fracability evaluation in naturally fractured sandstone reservoirs based on analytical hierarchy process method. *Energy Sci. Eng.* **2019**, *7*, 529–545. [[CrossRef](#)]
18. Ji, G.; Li, K.; Zhang, G.; Li, S.; Zhang, L. An assessment method for shale fracability based on fractal theory and fracture toughness. *Eng. Fract. Mech.* **2019**, *211*, 282–290. [[CrossRef](#)]
19. Zhou, X.; He, F.; Wei, J.G. A New Evaluation Procedure of Rock Fracability Using Cluster Analysis of Well-Logged Petrophysical Properties of Facies. *J. Min. Sci.* **2020**, *56*, 753–759.
20. Li, J.; Li, X.R.; Zhan, H.B.; Song, M.S.; Liu, C.; Kong, X.C.; Sun, L.-N. Modified method for fracability evaluation of tight sandstones based on interval transit time. *Pet. Sci.* **2020**, *17*, 477–486. [[CrossRef](#)]
21. Lu, C.; Ma, L.; Guo, J.; Li, X.; Zheng, Y.; Ren, Y.; Yin, C.; Li, J.; Zhou, G.; Wang, J.; et al. Novel method and case study of a deep shale fracability evaluation based on the brittleness index. *Energy Explor. Exploit.* **2022**, *40*, 442–459. [[CrossRef](#)]
22. Lutz, S.J.; Hickman, S.; Davatzes, N.; Zemach, E.; Drakos, P.; Robertson-Tait, A. Rock mechanical testing and petrologic analysis in support of well stimulation activities at the Desert Peak Geothermal Field, Nevada. In Proceedings of the 35th Workshop on Geothermal Reservoir Engineering, Stanford, CA, USA, 1–3 February 2010; pp. 373–380.
23. Holt, R.M.; Fjaer, E.; Nes, O.M.; Alassi, H.T. A shaly look at brittleness. In Proceedings of the 45th US Rock Mechanics/Geomechanics Symposium, San Francisco, CA, USA, 26–29 June 2011; ARMA-11-366.
24. Enderlin, M.B.; Alsleben, H.; Beyer, J.A. Predicting fracability in shale reservoirs. In Proceedings of the AAPG Annual Convention and Exhibition, Houston, TX, USA, 10–13 April 2011.
25. Mullen, M.; Enderlin, M. Fracability Index-more than just calculating rock properties. In Proceedings of the SPE Annual Technical Conference and Exhibition, San Antonio, TX, USA, 8–10 October 2012; SPE-159755-MS.
26. Yuan, J.; Zhou, J.; Liu, S.; Feng, Y.; Deng, J.; Xie, Q.; Lu, Z. An improved fracability-evaluation method for shale reservoirs based on new fracture toughness-prediction models. *SPE J.* **2017**, *22*, 1704–1713. [[CrossRef](#)]
27. Grieser, W.V.; Bray, J.M. Identification of production potential in unconventional reservoirs. In Proceedings of the Production and Operations Symposium, Oklahoma City, OK, USA, 31 March–3 April 2007; SPE-106623-MS.
28. Rickman, R.; Mullen, M.J.; Petre, J.E.; Grieser, W.V.; Kundert, D. A practical use of shale petrophysics for stimulation design optimization: All shale plays are not clones of the Barnett Shale. In Proceedings of the SPE Annual Technical Conference and Exhibition, Denver, CO, USA, 21–24 September 2008; SPE-115258-MS.
29. Whittaker, B.N.; Singh, R.N.; Sun, G. Rock fracture mechanics. Principles, design and applications. *Dev. Geotech. Eng.* **1992**, *71*, 1–21.
30. Griffith, A.A. The phenomenon of rupture and flow in solids. *Phil. Trans. R. Soc. Lond. A* **1920**, *221*, 163–198.
31. Irwin, G. Analysis of stresses and strains near the end of cracking traversing a plate. *J. Appl. Mech.* **1957**, *24*, 361–364. [[CrossRef](#)]
32. Palaniswamy, K.K.W.G. On the problem of crack extension in brittle solids under general loading. *Mech. Today* **1978**, *4*, 87–148.
33. Jin, Y.; Chen, M.; Zhang, X. Determination of fracture toughness for deep well rock with geophysical logging data. *Chin. J. Rock Mech. Eng.* **2001**, *20*, 454–456.
34. Jin, Y.; Yuan, J.; Chen, M.; Chen, K.P.; Lu, Y.; Wang, H. Determination of rock fracture toughness K_{IIC} and its relationship with tensile strength. *Rock Mech. Rock Eng.* **2011**, *44*, 621–627. [[CrossRef](#)]
35. Huang, R. A model for predicting formation fracture pressure. *J. East China Pet. Inst.* **1984**, *4*, 335–347.
36. Yu, X.; Wang, Y.; Li, Z. Calculation of horizontal principal in-situ stress with acoustic wave method. *Acta Pet. Sin.* **1996**, *17*, 59–63.
37. Holbrook, P. Discussion of a new simple method to estimate fracture pressure gradients. *SPE Drill. Completion* **1997**, *12*, 71.
38. Ge, H.K.; Lin, Y.S.; Ma, S.Z. Modification of Holbrook's fracture pressure prediction model. *Pet. Drill. Tech.* **2001**, *29*, 20–22.
39. Amadei, B.; Swolfs, H.S.; Savage, W.Z. Gravity-induced stresses in stratified rock masses. *Rock Mech. Rock Eng.* **1988**, *21*, 1–20. [[CrossRef](#)]
40. Amadei, B.; Pan, E. Gravitational stresses in anisotropic rock masses with inclined strata. *Int. J. Rock Mech. Min. Sci. Geomech. Abstr.* **1992**, *29*, 225–236. [[CrossRef](#)]
41. Higgins, S.M.; Goodwin, S.A.; Bratton, T.R.; Tracy, G.W. Anisotropic stress models improve completion design in the Baxter Shale. In Proceedings of the SPE Annual Technical Conference and Exhibition, Denver, CO, USA, 21–24 September 2008; SPE-115736-MS.
42. Khan, S.; Ansari, S.; Han, H.; Khosravi, N. Importance of Shale Anisotropy in Estimating In-Situ Stresses and Wellbore Stability Analysis in Horn River Basin. In Proceedings of the Canadian Unconventional Resources Conference, Calgary, AB, Canada, 15–17 November 2011; SPE-149433-MS.
43. Song, L.; Liu, Z.; Li, C.; Hu, S. Geostress logging evaluation method of tight sandstone based on transversely isotropic model. *Acta Pet. Sin.* **2015**, *36*, 707–714.
44. Lamont, N.; Jessen, F.W. The effects of existing fractures in rocks on the extension of hydraulic fractures. *J. Pet. Technol.* **1963**, *15*, 203–209. [[CrossRef](#)]
45. Daneshy, A.A. Hydraulic fracture propagation in the presence of planes of weakness. In Proceedings of the SPE European Spring Meeting, Amsterdam, The Netherlands, 29–30 May 1974; SPE-4852-MS.

46. Blanton, T.L. An experimental study of interaction between hydraulically induced and pre-existing fractures. In Proceedings of the SPE Unconventional Gas Recovery Symposium, Pittsburgh, PA, USA, 16–18 May 1982; SPE-10847-MS.
47. Warpinski, N.R.; Teufel, L.W. Influence of geologic discontinuities on hydraulic fracture propagation. *J. Pet. Technol.* **1987**, *39*, 209–220. [[CrossRef](#)]
48. Renshaw, C.E.; Pollard, D.D. An experimentally verified criterion for propagation across unbounded frictional interfaces in brittle, linear elastic materials. *Int. J. Rock Mech. Min. Sci. Geomech. Abstr.* **1995**, *32*, 237–249. [[CrossRef](#)]
49. Zhou, J.; Chen, M.; Jin, Y.; Zhang, G.Q. Analysis of fracture propagation behavior and fracture geometry using a tri-axial fracturing system in naturally fractured reservoirs. *Int. J. Rock Mech. Min. Sci.* **2008**, *45*, 1143–1152. [[CrossRef](#)]
50. Cheng, W.; Jin, Y.; Chen, M.; Xu, T.; Zhang, Y.; Diao, C. A criterion for identifying hydraulic fractures crossing natural fractures in 3D space. *Pet. Explor. Dev.* **2014**, *41*, 371–376. [[CrossRef](#)]
51. Cheng, W.; Jin, Y.; Chen, M.; Zhang, Y.; Xi, C.; Hou, B. Experimental investigation on influence of discontinuities on hydraulic fracture propagation in three-dimensional space. *Chin. J. Geotech. Eng.* **2015**, *37*, 559–563.
52. Dou, L.; Yang, M.; Gao, H.; Jiang, D.; Liu, C. Characterization of the dynamic imbibition displacement mechanism in tight sandstone reservoirs using the NMR technique. *Geofluids* **2020**, *2020*, 8880545. [[CrossRef](#)]
53. Dou, L.; Xiao, Y.; Gao, H.; Wang, R.; Liu, C.; Sun, H. The study of enhanced displacement efficiency in tight sandstone from the combination of spontaneous and dynamic imbibition. *J. Pet. Sci. Eng.* **2021**, *199*, 108327. [[CrossRef](#)]